https://doi.org/10.61092/iaea.vr5w-1y0s
INDC(NDS)-0789
Distr. AD,G,IN,J,RD

IAEA
International Atomic Energy Agency

INDC International Nuclear Data Committee

IAEA Coordinated Research Project F41031: Testing and Improving the IAEA International Reactor Dosimetry and Fusion File (IRDFF)

Final Report

M. Majerle[1], M. Ansorge[1], P. Bém[1], J. Novák[1], E. Šimečková[1], M. Štefánik[1]
1) Nuclear Physics Institute of the CAS PRI, 250 68 Řež, Czech Republic

May 2019

IAEA Nuclear Data Section
Vienna International Centre, P.O. Box 100, 1400 Vienna, Austria

Selected INDC documents may be downloaded in electronic form
from *http://nds.iaea.org/publications*
or sent as an e-mail attachment.
Requests for hardcopy or e-mail transmittal should be directed to
NDS.Contact-Point@iaea.org
or to:
Nuclear Data Section
International Atomic Energy Agency
Vienna International Centre
PO Box 100
1400 Vienna
Austria

Printed by the IAEA in Austria
May 2019

IAEA Research Contract No: 17794

IAEA Coordinated Research Project F41031: Testing and Improving the IAEA International Reactor Dosimetry and Fusion File (IRDFF)

Final Report

Experimental Validation of IRDFF Cross-Sections in Quasi-MonoEnergetic Neutron Fluxes in 20-35 MeV Energy Range

M. Majerle[1], M. Ansorge[1], P. Bém[1], J. Novák[1], E. Šimečková[1], M. Štefánik[1]
1) Nuclear Physics Institute of the CAS PRI, 250 68 Řež, Czech Republic

August 2018

1 Introduction

The International Reactor Dosimetry and Fusion File (IRDFF-v1.05) is a standardized evaluated cross section library of neutron dosimetry reactions and uncertainty information that supersedes the widely used IRDF-2002 library [1,2]. The improvements over IRDF-2002 are between others the extension of the upper energy range from 20 MeV to 60 MeV and the inclusion of several new dosimetry reactions.

It is a known fact that experimentally obtained cross-section data are rare and uncertain especially above the neutron energy of 20 MeV. Several introduced evaluations therefore need additional validations based on new and less uncertain differential cross-section measurements.

The goal of this work is to validate the cross-sections for reactions (n,xn/p/α) on ^{197}Au, ^{209}Bi, ^{59}Co, ^{54}Fe and ^{169}Tm in the energy range 20-35 MeV. The following reactions are commonly used to monitor the intermediate energy neutron flux and spectrum, and their cross-sections are included in the IRDFF: ^{197}Au(n,2n)$^{196g+m+m2}$Au, ^{209}Bi(n,3n)^{207}Bi, ^{59}Co(n,2n)$^{58g+m}$Co, ^{59}Co(n,3n)^{57}Co, ^{54}Fe(n,2n)^{53}Fe, ^{54}Fe(n,p)^{54}Mn, ^{54}Fe(n,α)^{51}Cr, ^{169}Tm(n,2n)^{168}Tm, ^{169}Tm(n,3n)^{167}Tm. The validation is achieved through irradiation of the target materials in a well-known neutron spectrum, subsequent gamma-spectroscopy measurements of the produced nuclei and the comparison of the newly measured cross-section data with the contents of other evaluations.

The Department of Nuclear Reactions of the NPI has long-term expertise in this type of the measurements. The measurement of the neutron cross-sections above 20 MeV relevant on the elements important for fusion and accelerator driven facilities have been performed and already published [3-7].

2 Main parameters of the experiments

2.1 Quasi-monoenergetic neutron generator at the NPI

The neutron irradiations (20-35 MeV range) have been performed at the NPI quasi-monoenergetic neutron generator based on the p+^{7}Li reaction. Protons were directed at a 2 mm thick lithium foil with a 1 cm carbon backing, which fully stopped the protons and allowed to irradiate the samples close to the neutron production target where the neutron intensity is high. A detailed description of the experimental setup and procedures is presented in [5]. A number of incident proton energies were used between 20-35 MeV (Tables 1-2). 99.9% enriched ^{7}Li foil was used for all irradiations, with the exception of the repeated irradiations at 25 and 27.5 MeV proton energy at which ^{nat}Li foil was used. A new Li foil was used at each irradiation, the irradiated Li foil was used for the spectroscopic analysis of the produced ^{7}Be in the target and stored in oil. The energy spread of the proton beam was estimated to have the Gaussian distribution with FWHM=200 keV, the absolute energy of protons is defined with the accuracy of 1.5%.

The irradiated samples of ^{197}Au, ^{209}Bi, ^{59}Co, ^{nat}Fe and ^{169}Tm in the form of thin foils with disc shape (diameter 15 mm) were placed 86-87 mm from the lithium target front. In all experiments the samples were arranged with other activation samples in the following order: ^{169}Tm (thickness 0.1mm), ^{197}Au (0.05mm), ^{nat}Fe (0.25mm), ^{nat}W (0.025mm) ^{59}Co (0.25mm), and ^{209}Bi (1.5mm). The absorption of neutrons in the samples was negligible (determined with MCNPX simulations). The samples were weighted at an absolute accuracy below 0.5%. New samples (not previously irradiated) were used at each irradiation.

The samples were irradiated during 6-8 hours. The irradiation intensity was recorded by measuring the proton current at the target assembly at a time scale of 1 second and the correction for the beam instabilities was included in the calculation of the reaction rates. In the case of ^{53}Fe with the decay time of 8.51 minutes, the samples were repeatedly irradiated for ca. 5 minutes and transported in front of the HPGe detector using the pneumatic post system to avoid the delay and decay of the produced ^{53}Fe.

At each irradiation, the Time-Of-Flight (TOF) spectrum was recorded using a 2"x2" NE213 scintillator placed at the distance of 4.5 m from the target front on the beam axis. The absolute number of forward directed peak neutrons was extracted. The integral number of the produced peak neutrons was determined from the offline γ-spectroscopy measurements of the activity of ^{7}Be isotope produced in the lithium target using the HPGe detectors.

2.2 HPGe measurements

Several radioactive products were detected in the neutron irradiated samples and lithium foils by the offline γ-spectroscopy employing calibrated HPGe detectors with the efficiency around 50%-NPI and good energy resolution (FWHM=1.3-1.8 keV). The decay γ-spectra were measured during the cooling period from minutes up to 100 days. The gamma intensities were taken from the ENSDF database (evaluation from 2007) [8]. The disagreement between the tabulated intensities and measured surfaces under the peaks was observed for the isotope ^{196m2}Au. The detailed study of the γ-ray intensities from the decay of this isotope was performed [9] and according to these measurements the values 43% and 34.0% were used in this work as the intensities of the most intensive γ-ray transitions at 147.81 keV and 188.27 keV.
The reaction rates (the number of produced residual nuclei per number of atoms in the sample and per number of incident protons) were calculated from the measured areas of the γ-peaks using all standard spectroscopic corrections and are presented in the Table 1. Where available, the averaged values obtained from previous irradiations in the same position are also shown for comparison. All reaction rates are normalized to the measured value of the proton charge (the produced number of ^{7}Be nuclei was measured using the HPGe detector, it gives accurate information on the total number of peak neutrons and is also normalized per proton charge, see Table 2). The uncertainties given in the Table 1 include the uncertainty of the peak surface fitting, of the HPGe detector calibration (below 2%) and of the subtraction of the contribution

from other isotopes or background. By comparing the results from this work with the reaction rates from previous irradiation campaigns we determined the repeatability of the measured reaction rates to be between 5 and 10%. The results from this work come with more precisely determined number of the peak neutrons (^{7}Be activity measurements, Table 2) which were used in the neutron spectrum normalization and subsequently in the cross-section extraction procedure.

Proton energy [MeV]/reaction	20	22.5	25 (^{7}Li)	25 (^{nat}Li)	27.5 (^{7}Li)	27.5 (^{nat}Li)	30	32.5	35
^{197}Au(n,2n)$^{196g+m1+m2}$Au Previous work	100±2% 98±3%	103±2% 105±4%	90±2% 84±3%		96±2% 98±4%		118±2% 116±3%	139±2% 122±5%	180±2% 171±5%
^{209}Bi(n,3n)^{207}Bi(x10^{-4}) Previous work (x10^{-4})	117±13%	344±8% 271±3%	607±6%		731±6% 678±3%		749±4%	626±6% 663±5%	635 ±8% 520±3% @36.5 MeV
^{59}Co(n,2n)$^{58g+m}$Co Previous work	11.8±2% 10.5±3%	15.3±2% 17.6±3%	17.8±2% 16.9±4%	14.7±3%	19.6±2% 18.3±3%	16.0±3%	17.1±2% 17.9±3%	18.8±2% 20.6±3%	20.9±2% 22.1±4%
^{59}Co(n,3n)^{57}Co (x10^{2}) Previous work(x10^{2})		0.4±25%	21.6±2% 23.4±3%	16.0±2%	102±2% 96.7±3%	74.6±2%	157±2% 163±3%	205±2% 198±3%	221±2% 213±3%
^{59}Co(n,p)^{59}Fe Previous work	1.38±2% 1.34±3%	1.48±2%	1.59±2% 1.64±3%	1.33±2%	2.07±2% 1.87±3%	1.69±2%	2.14±2% 2.38±3%	2.80±2% 2.77±3%	3.39±2% 3.41±3%
^{59}Co(n,α)^{56}Mn Previous work	279±2% 268±3%	271±2%	268±2% 261±3%	219±2%	 282±3%	261±2%	313±2% 338±3%	400±2% 405±4%	502±2% 505±3%
^{nat}Fe(n,2n)^{53}Fe	1500±3%	2450±2%	3790±2%	2960±2%		5010±2%	4920±3%	4930±3%	5690±2%
^{nat}Fe(n,p)^{54}Mn (x10^{2})	16.8±3%	16.2±7%	17.8±3%	11.4±5%	35.7±11 %	25.7±3%	77.2±2%	139±2%	200±2%
^{nat}Fe(n,α)^{51}Cr (x10^{2})	35.2±15 %	24.1±6%	22.3±9%	16.7±5%	23.8±12 %	20.6±7%	28.8±10 %	83.1±4%	205±2%
^{169}Tm(n,2n)^{168}Tm	6.63±3%	6.69±3%	6.14±6%		6.52±3%		7.4±4%	9.27±3%	11.8±5%
^{169}Tm(n,3n)^{167}Tm	10.0±10 %	44.8±8%	83±8%		96.8±9%		110±9%	96±7%	85±6%

Table 1: Experimental reaction rates in the irradiated foils measured after the irradiation with the quasi-monoenergetic neutrons from the p+Li reaction at the NPI. The thickness of the lithium converter was 2 mm, distance of the irradiation position from the target front was 86-87 mm. The reaction rates are calculated for the end of the irradiation time and are expressed in [Bq/kg/μC]. This table is normalized per proton charge that was deposited on the target station, but accurate information on the number of produced peak neutrons is available in Table 2 from ^{7}Be activity measurements. The reaction rates averaged from previous experiments (performed in years 2009-2013 - [5]) are shown where available in red.

Proton energy [MeV]	N(^{7}Be in 2mm Li) (x10^{14})
19.8	20.0±4%
22.4	18.5±4%
25.1 (^{7}Li)	17.0±4%
25 (^{nat}Li)	12.7±4%
27.5 (^{7}Li)	No data
27.67 (^{nat}Li)	12.6±4%
30.4	12.9±4%
32.5	10.6±4%
35.0	10.9±4%

Table 2: The production of ^{7}Be in 2 mm Li foil irradiated with protons at an energy range 20-35 MeV at the NPI. The discrepancies from the smooth trend are connected with the foil thickness uncertainty (5%) and in the case of the ^{nat}Li foils with the amount of Li in the foil. The good quality ^{7}Li foils were from the same provider (Russia, side product from ^{6}Li extraction), ^{nat}Li foils were provided by Goodfellow (large discrepancies from the expected number of ^{7}Be were observed also at other irradiations of Goodfellow produced ^{nat}Li foils).

3 Determination of the produced neutron spectrum in the irradiation position

3.1 Experimental data on the forward directed neutrons

Schery et al. suggested to use the measurement of the ^{7}Be production in the lithium target to determine the total number of produced peak neutrons in the reaction ^{7}Li(p,n)^{7}Be [10].

The experimental data for ^{7}Be production available in EXFOR shows a good agreement and a nice trend in the energy range 20-60 MeV. The best fit to the data was obtained with the curve:

$$\sigma(E) = 36.5658\, e^{-0.5\left(\frac{E+455.914}{126.689}\right)^{2}}$$

The number of the produced ^{7}Be nuclei was measured for all irradiations (with the exception of the 27.5 MeV irradiation of ^{7}Li target, Table 2), the total number of the peak neutrons was therefore determined. Only, in the case of the 27.5 MeV irradiation of the ^{7}Li foil, the production of the peak neutrons was deduced from the fitted curve.

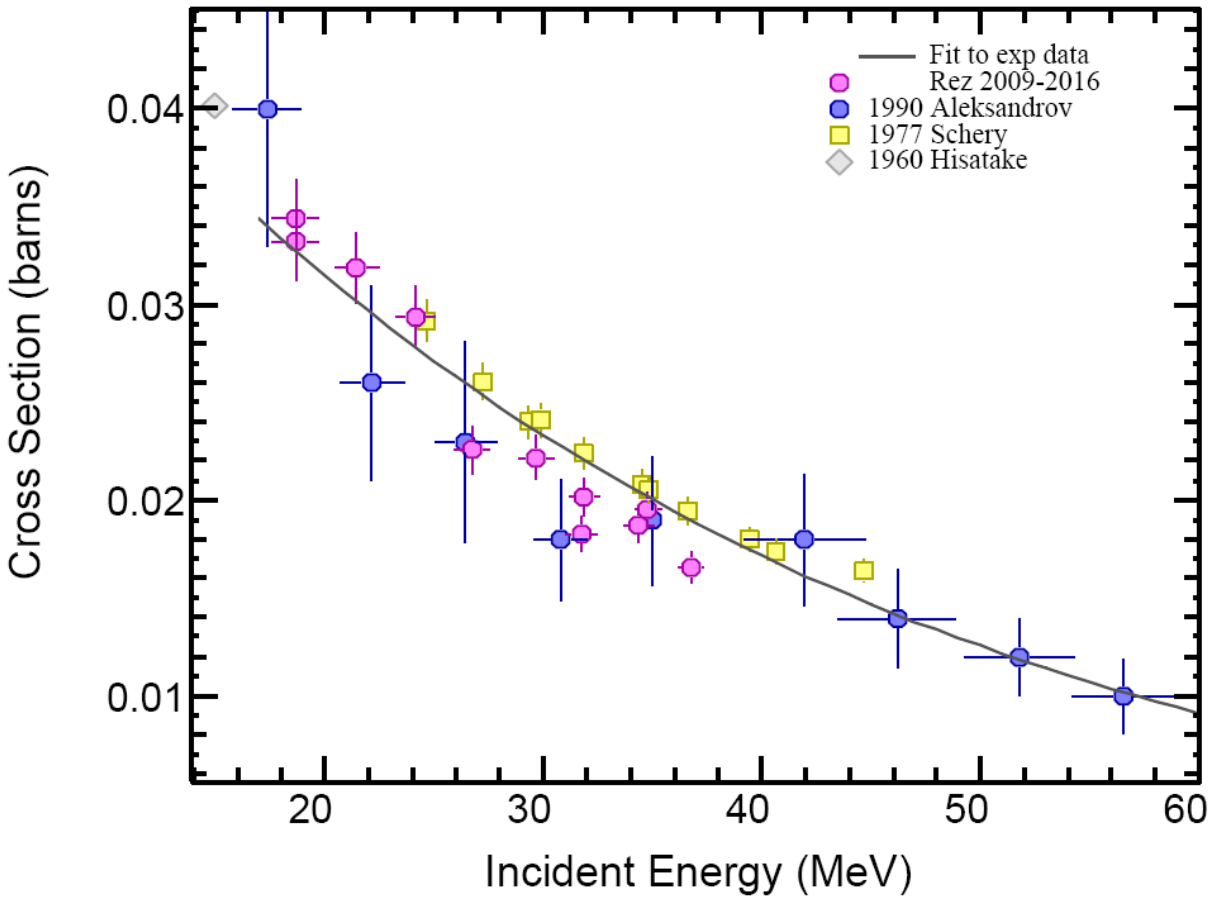

Figure 1 - The EXFOR cross-section data of the ^{7}Li(p,n)^{7}Be reaction compared with our data measured in the time period 2009-2016 [5]. Good agreement with other data sets is obtained. The fit curve of the experimental data is also shown.

The ratio between the number of the peak neutrons in the forward direction and total number of the peak neutrons was established by Uwamino [11]. He integrated the angular cross-sections of the peak neutrons from his own measurements and angular distributions measured by Schery [10]. We extended his set of angular cross-section integrations with the data sets by Batty [12], Orihara [13] and Poppe [14] (by integrating their angular distributions) and our own measurements. We have measured independently the absolute number of forward directed neutrons using the NE213 scintillator in the TOF mode and the total number of the peak neutrons using γ-spectrometry to determine the ^{7}Be production in the lithium target. All the data points are shown together with the curves for ratios calculated from the Uwamino formula and the curve valid for the Tadeucci systematics (obtained with the integration of the angular distribution, valid above 80 MeV) [15]. All the experimental data confirm the validity of the Uwamino formula in the energy range below 45 MeV.

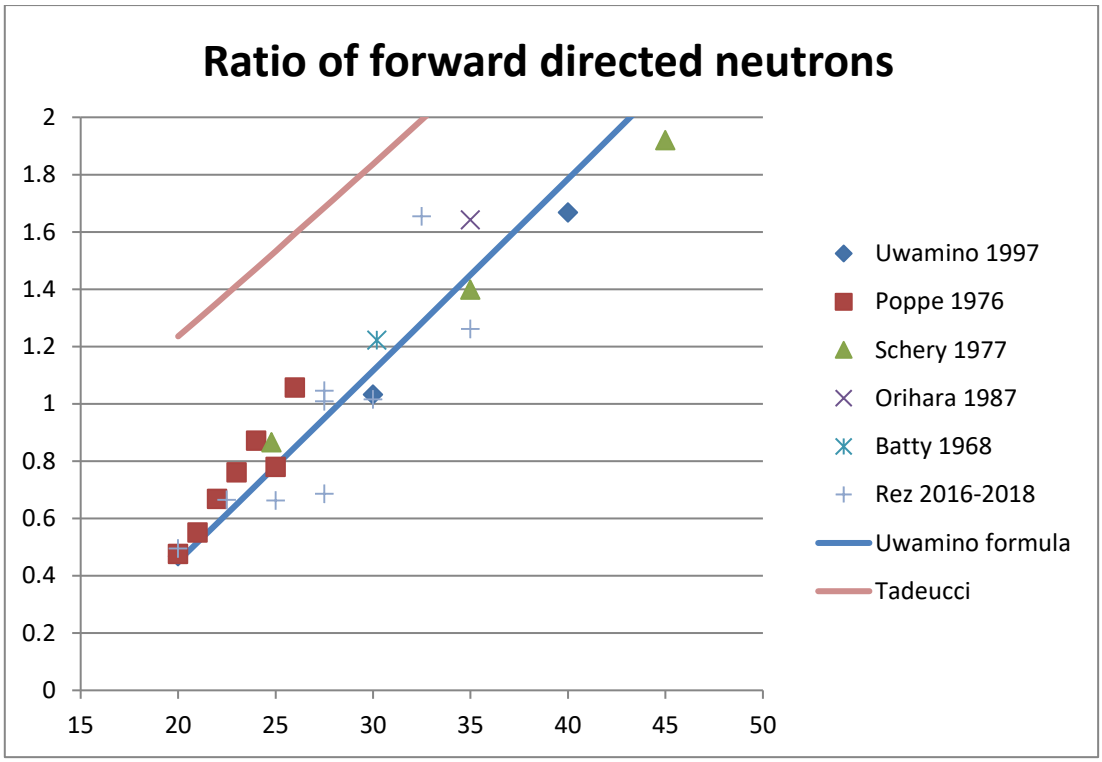

Figure 2 - The experimental data on the ratio of the forward directed peak neutrons. The data points from Uwamino, Schery, Batty, Poppe and Orihara have been calculated from their results on the angular distribution of the peak neutrons. The data from Řež were obtained as the ratio of independent measurements of forward directed peak neutrons with the NE213 scintillator and of the number of produced ^{7}Be nuclei with the HPGe detector. The curve from the Tadeucci systematics is shown from completeness.

3.2 Neutron spectrum determination

The neutron spectral shape could not be satisfactory measured at the irradiation position (86-87 mm from the target front). The precise measurements of the neutron spectra at the positions where the samples are irradiated are impossible and the TOF measurements of the neutron spectra are performed at larger distances (5m) from the target. To extrapolate the measured data about the neutron spectra to the position where the samples were irradiated and to account for possible contribution of scattered neutrons, we used the MCNPX code [16] with the appropriate neutron production library and subsequent normalization of the simulated results based on the experimental data.

We validated this approach versus our experimental data measured by TOF and ^{7}Be production and experimental data by other authors [5]. Two evaluations of neutron production from the p+^{7}Li reaction are available: LA150H [17] and JENDL-4.0/HE [18]. We were using the LA150H evaluation in our previous work with the renormalization of the spectra based on the number of peak neutrons (determined from measured ^{7}Be production and Uwamino formula for the ratio of forward directed neutrons) in the range of 0.8-1.3. The simulations showed that the contribution of the scattered neutrons at the irradiation position can be neglected and that the absorption of neutrons in the

target station material is from 10-15% depending on the proton energy. The JENDL-4.0/HE evaluation was as well used to simulate the neutron production at both facilities. In this evaluation, the newest data on the ^{7}Be production from EXFOR are included and the angular description of the peak neutrons is derived from the new Legendre fits of the available experimental data. The same conclusions as in the case of the LA150H library were drawn for the contribution of the scattered neutrons and absorption of the neutrons in the target station material.

As for the number of forward directed peak neutrons, none of these two libraries provides data in good agreement with the experiment (using ^{7}Be production measured by γ-spectrometry and Uwamino formula for the ratio of the forward directed neutrons). The simulated spectra were therefore additionally normalized using the approach described below.

Considering all this, the neutron spectra at the irradiation position and in the forward direction (angle 0.5 degrees was used for sampling) were simulated with the MCNPX code (two sets of the spectra using libraries LA150H and JENDL-4.0/HE were produced for comparison of the extracted cross-sections). The simulated number of peak neutrons in the forward direction and the Uwamino formula were used to calculate the total number of peak neutrons in the simulation (the spectra were corrected for the absorption of the neutrons in the target station material, mainly carbon beam stopper, spectra were divided with 0.86-0.90 – obtained using MCNPX simulations). The simulated number of peak neutrons was compared with the measured number of the produced ^{7}Be nuclei (or fit result for the 27.5 MeV irradiation at the NPI) and the renormalization constant was calculated. The spectra at the irradiation position were then renormalized using this constant. The final spectra that were used in the extraction procedure are shown in Figures 3 and 4.

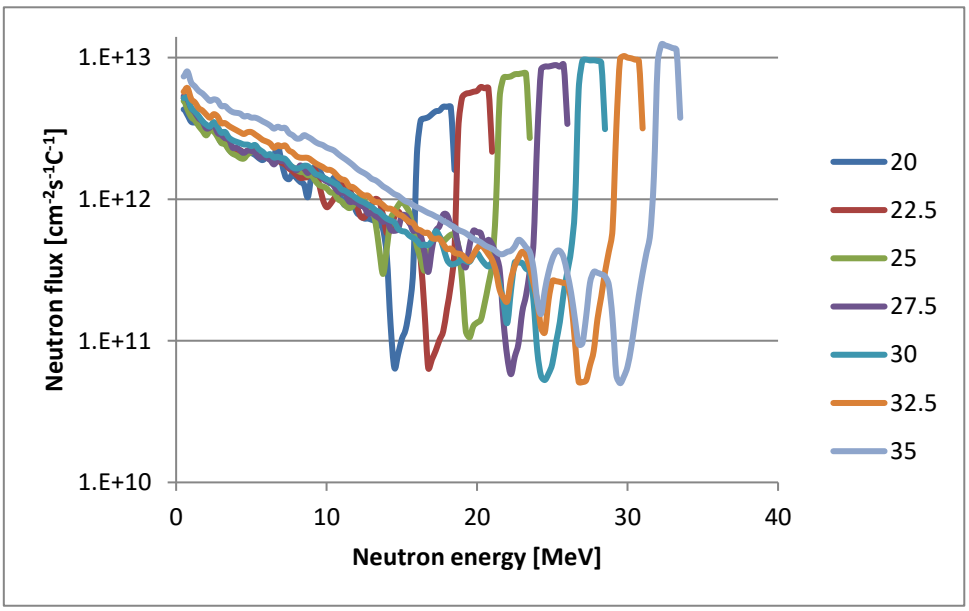

Figure 3 - The neutron spectra at the irradiation position for different proton beam energies (20-35 MeV). Spectra were calculated with the MCNPX code using LA150H library and renormalized as described in the text. The distance from the target front to the irradiation position is 8.6 cm.

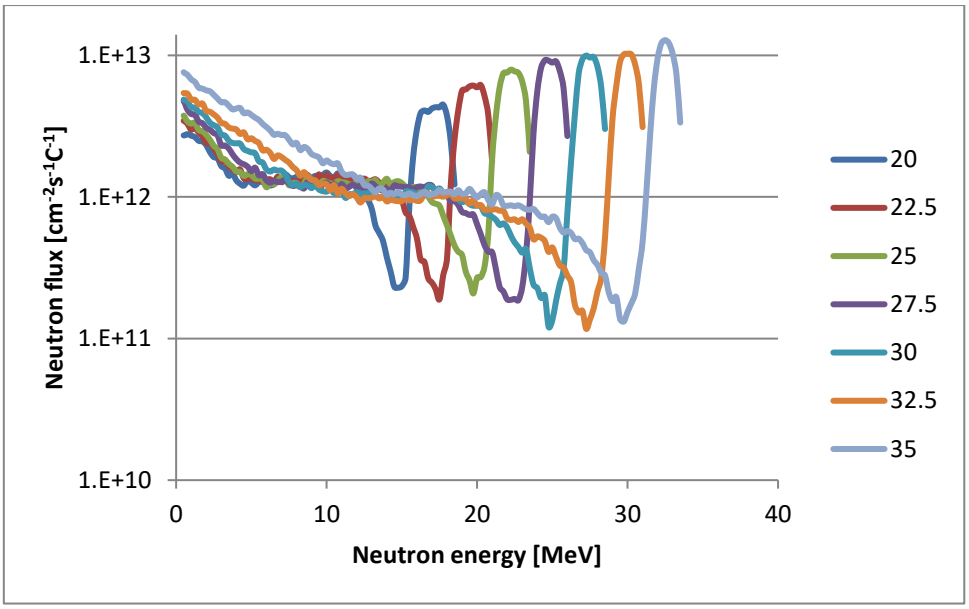

Figure 4 - The neutron spectra at the irradiation position for different proton beam energies (20-35 MeV). Spectra were calculated with the MCNPX code using JENDL-4.0/HE library and renormalized as described in the text. The distance from the target front to the irradiation position is 8.6 cm.

4 Extraction of cross-section

4.1 Cross-section extraction procedure

The neutron spectrum at the irradiation position consists of the monoenergetic peak and the continuum at lower energies. To derive the activation cross-sections curves in the complex neutron field a modified version of the SAND-II [19] code was used. The procedure is described in details in [5]. The neutron spectra, cross-section curve from the IRDFF v1.05 evaluation (processed with PREPRO tools [20]) and measured reaction rates are used as input parameters. In the case of several isotopes in the studied material, the according cross-sections were multiplied with the abundance of the reacting isotope (^{54}Fe in ^{nat}Fe).
The SAND-II code iteratively justifies the cross-section curve until the agreement between the measured reaction rates and the reaction rates calculated by folding the neutron spectra with the cross-section curve is reached. The obtained cross-section curve is averaged at the energy regions covered with monoenergetic peaks, the averaged values are presented as extracted cross-sections. The uncertainty of the cross-section on the energy scale is determined with the energy width of the monoenergetic neutrons, on the cross-section scale the uncertainty is calculated from the quadratic sum of the uncertainties of the reaction rates and the uncertainty of the extraction procedure. The latter uncertainty is defined as the difference that is obtained with the same extraction procedure using different sets of neutron spectra (LA150H and JENDL-4.0/HE), see Figure 5.

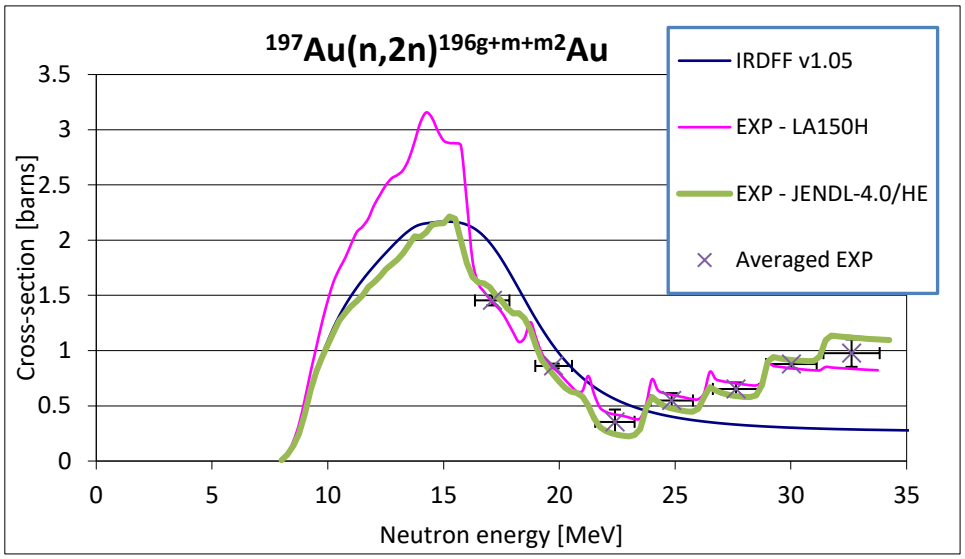
197Au(n,2n)196g+m+m2Au
IRDFF v1.05
EXP - LA150H
EXP - JENDL-4.0/HE
Averaged EXP
Cross-section [barns]
Neutron energy [MeV]
0
0.5
1
1.5
2
2.5
3
3.5
0
5
10
15
20
25
30
35

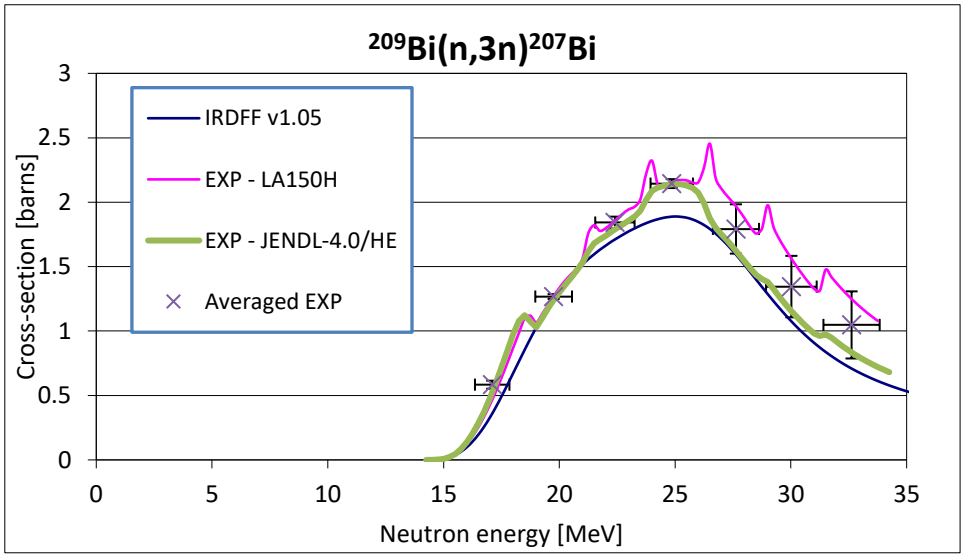
209Bi(n,3n)207Bi
IRDFF v1.05
EXP - LA150H
EXP - JENDL-4.0/HE
Averaged EXP
Cross-section [barns]
Neutron energy [MeV]
0
0.5
1
1.5
2
2.5
3
0
5
10
15
20
25
30
35

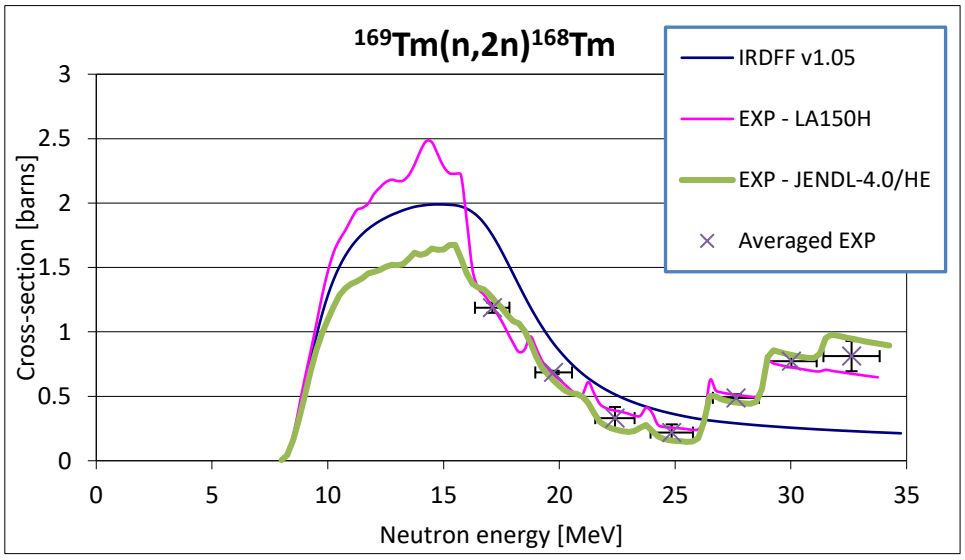
169Tm(n,2n)168Tm
IRDFF v1.05
EXP - LA150H
EXP - JENDL-4.0/HE
Averaged EXP
Cross-section [barns]
Neutron energy [MeV]
0
0.5
1
1.5
2
2.5
3
0
5
10
15
20
25
30
35

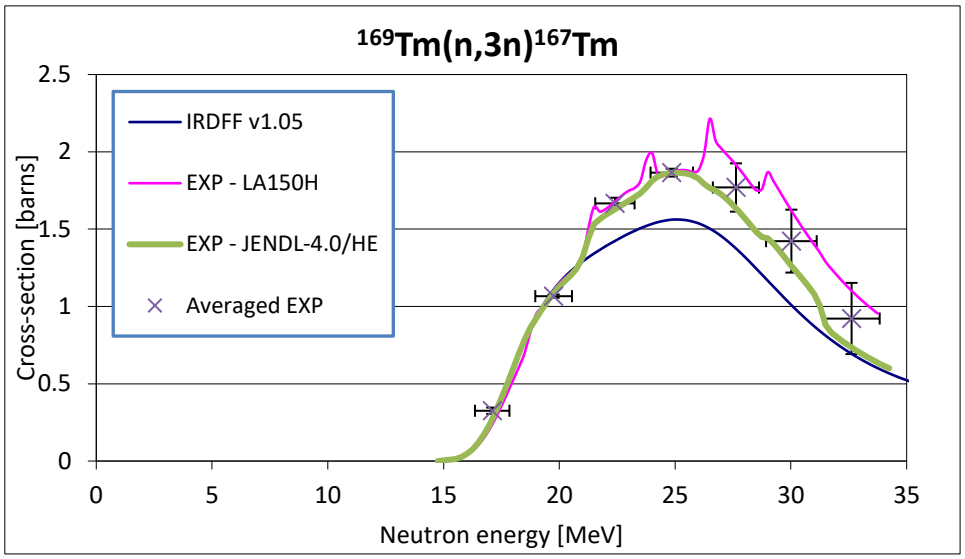
169Tm(n,3n)167Tm
IRDFF v1.05
EXP - LA150H
EXP - JENDL-4.0/HE
Averaged EXP
Cross-section [barns]
Neutron energy [MeV]
0
0.5
1
1.5
2
2.5
0
5
10
15
20
25
30
35

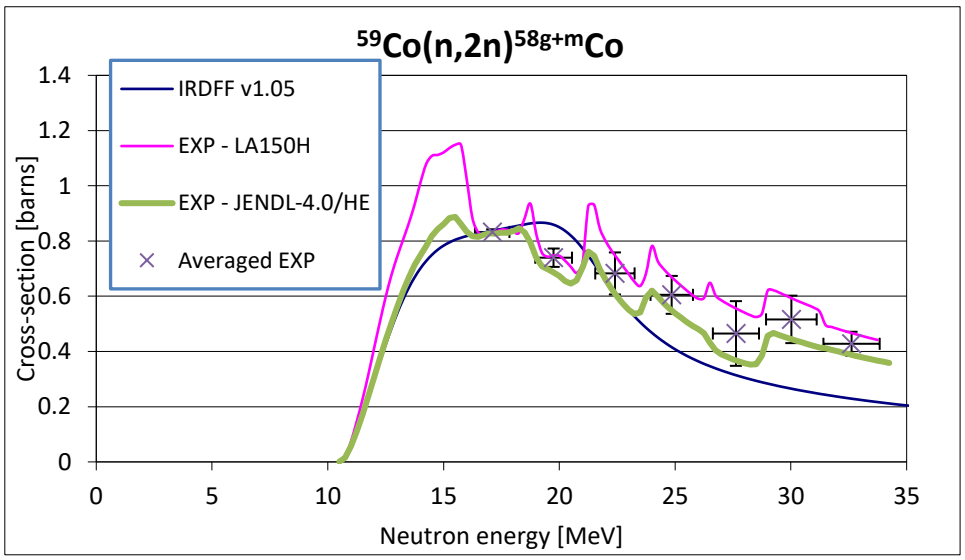
59Co(n,2n)58g+mCo
IRDFF v1.05
EXP - LA150H
EXP - JENDL-4.0/HE
Averaged EXP
Cross-section [barns]
Neutron energy [MeV]
0
0.2
0.4
0.6
0.8
1
1.2
1.4
0
5
10
15
20
25
30
35

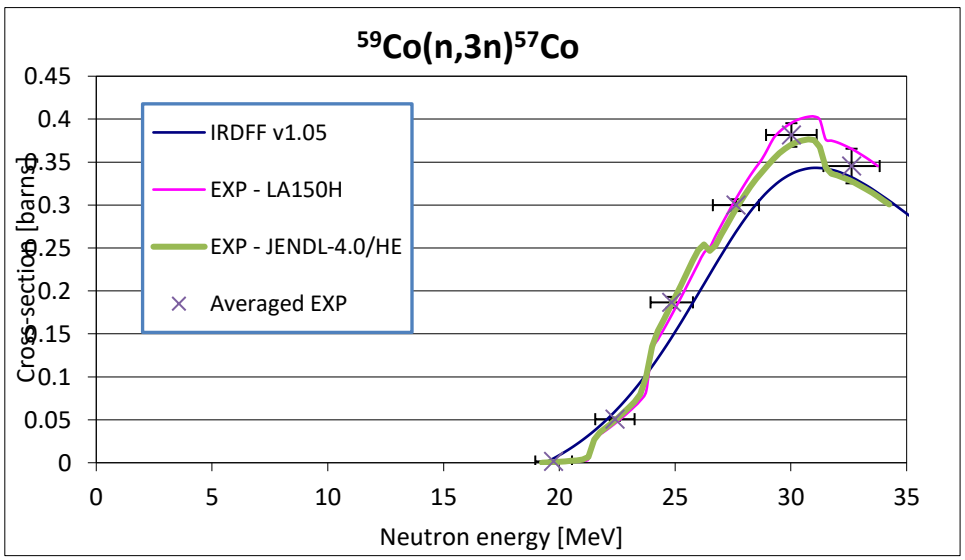
59Co(n,3n)57Co
IRDFF v1.05
EXP - LA150H
EXP - JENDL-4.0/HE
Averaged EXP
Cross-section [barns]
Neutron energy [MeV]
0
0.05
0.1
0.15
0.2
0.25
0.3
0.35
0.4
0.45
0
5
10
15
20
25
30
35

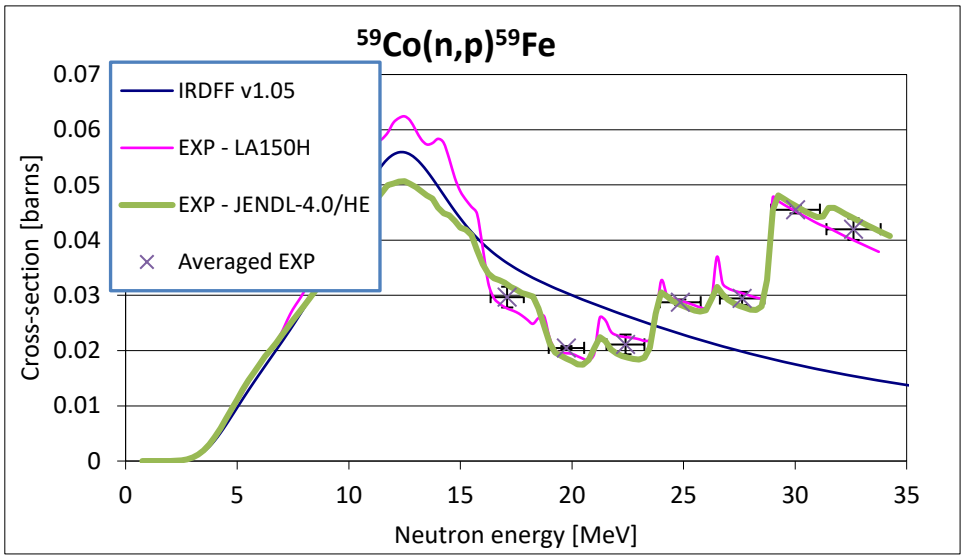
59Co(n,p)59Fe
IRDFF v1.05
EXP - LA150H
EXP - JENDL-4.0/HE
Averaged EXP
Cross-section [barns]
Neutron energy [MeV]
0.07
0.06
0.05
0.04
0.03
0.02
0.01
0
0
5
10
15
20
25
30
35

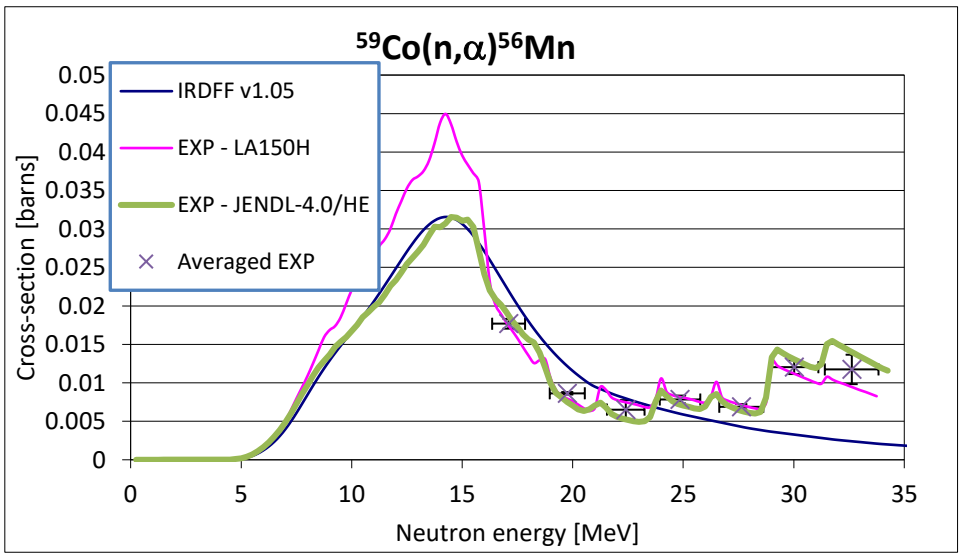
59Co(n,α)56Mn
IRDFF v1.05
EXP - LA150H
EXP - JENDL-4.0/HE
Averaged EXP
Cross-section [barns]
Neutron energy [MeV]
0.05
0.045
0.04
0.035
0.03
0.025
0.02
0.015
0.01
0.005
0
0
5
10
15
20
25
30
35

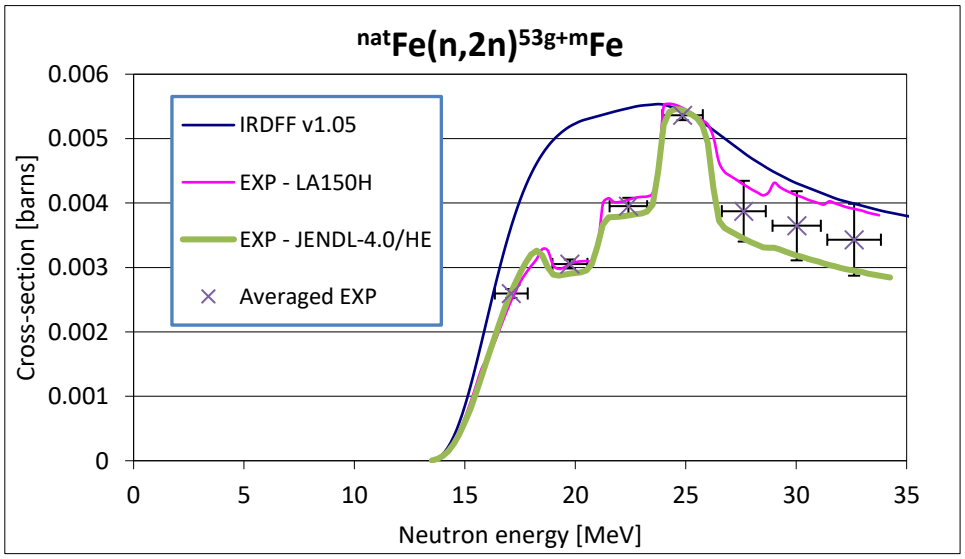
natFe(n,2n)53g+mFe
IRDFF v1.05
EXP - LA150H
EXP - JENDL-4.0/HE
Averaged EXP
Cross-section [barns]
Neutron energy [MeV]
0.006
0.005
0.004
0.003
0.002
0.001
0
0
5
10
15
20
25
30
35

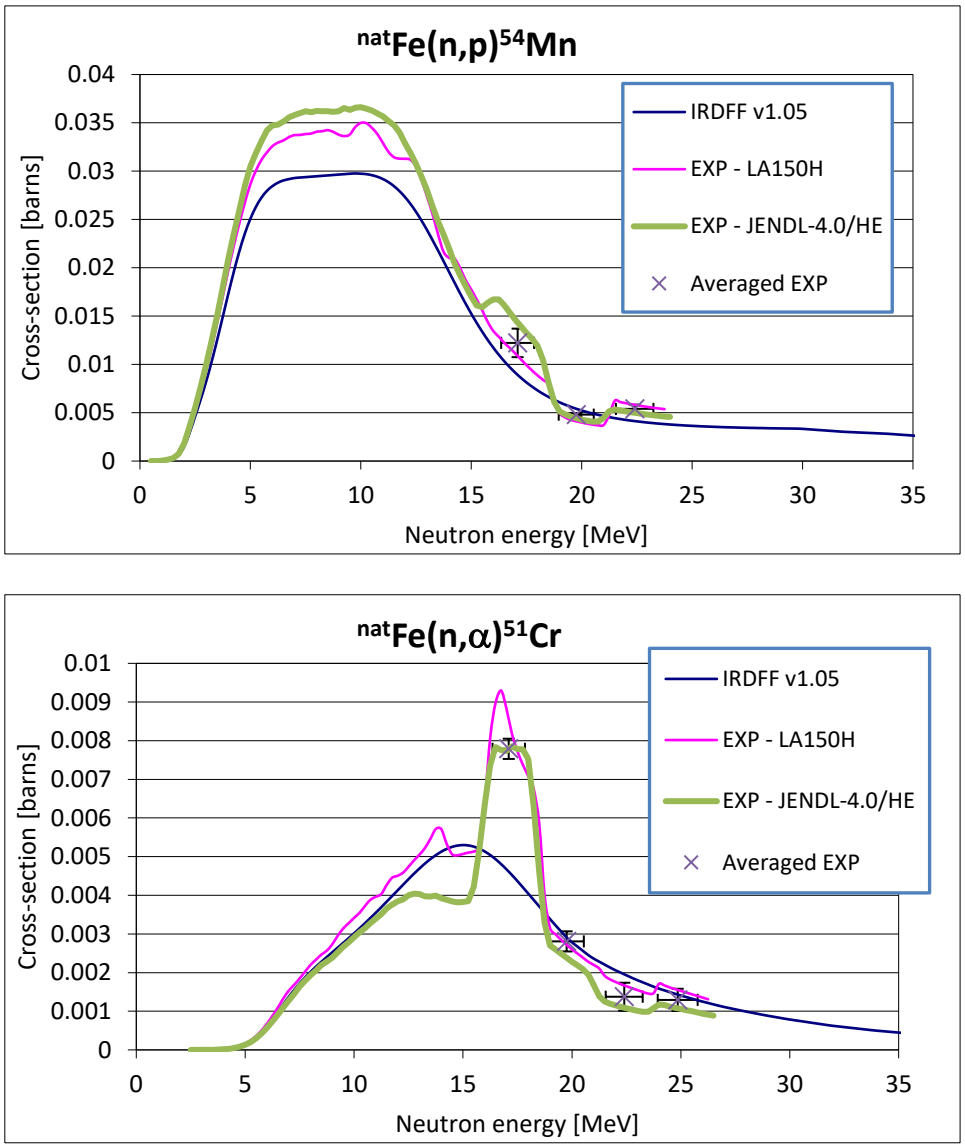

Figure 5 - The cross-sections curves extracted with SAND-II using the input cross-sections from the IRDFF v1.05 evaluation and neutron spectra from Figures 3-4. The values at the regions defined by monoenergetic peak neutrons are averaged and presented as the experimental results. The uncertainties on the cross-section scale include the uncertainties of the measured reaction rates and the difference between the cross-section curves produced using two different sets of calculated neutron spectra (LA150H and JENDL-4.0/HE).

4.1 Extracted cross-sections

A general trend of the disagreement of experimental values with the evaluation can be observed. The experimental values at lower energies (first 3-4 values) agree with the evaluation while those at higher energies are significantly larger than the evaluation. The uncertainty (defined mainly by the difference made by using two different neutron spectra) also increases at higher energies. By several custom variations of the input neutron spectra it was determined that the problem lies in the subtraction of the

contribution of neutrons from the continuum (neutron below the monoenergetic peak). This effect is more expressed at reactions with lower thresholds - reactions (n,2n), (n,p), (n,α).

The experimental values where the contribution of the neutrons below the monoenergetic peak is large, should therefore not be considered reliable.

5 Conclusion

A new set of measured experimental values of reaction rates agrees with the previously measured data within 5-10%. For the newly measured values the accurate number of peak neutrons was determined using the γ-spectrometry (^{7}Be production in the lithium target). The Uwamino formula for the forwardness of the peak neutrons was validated with sets of experimental data newly available at EXFOR and our own measurements. This formula together with the accurate experimental number of peak neutrons was used to normalize the spectra calculated by MCNPX using LA150H and JENDL-4.0/HE libraries (the number of the peak neutrons simulated in the forward directions were normalized to the experimentally determined number of peak neutrons multiplied with the ration of the forward directed neutrons).
Using two sets of the simulated and normalized neutron spectra, the cross-sections were extracted from the experimental reaction rates. The extracted cross-sections show a typical trend of disagreement at higher energies. With variations of the neutron spectra used in the extraction procedure, it was found that this disagreement comes from the subtraction of the contribution of the neutrons below monoenergetic peaks – continuum neutrons. Also, the largest contribution to the extracted cross-sections uncertainty comes from this subtraction.
A better knowledge of the neutron spectra at the irradiation positions is therefore necessary to improve the quality of the extracted cross-sections. Also measurements at different geometries (continuum subtraction by measuring at two angles) might be helpful.

References

1) R. Capote, K.I. Zolotarev, V.G. Pronyaev, and A. Trkov, J. ASTM International, Volume 9, Issue 4, April 2012, JAI104119. DOI: 10.1520/JAI104119

2) E.M.Zsolnay, R. Capote, H.K. Nolthenius, and A. Trkov, Technical report INDC(NDS)-0616, IAEA, Vienna, 2012.

3) M. Honusek, et al., “Neutron Activation Experiments on Niobium in NPI p-^{7}Li Quasi-monoenergetic Neutron Field”, Journal of the Korean Physical Society, Vol. 59, No. 2, August 2011, pp. 13741377, DOI: 10.3938/jkps.59.1374

4) E. Simeckova, et al., “The Measurement of Neutron Activation Cross Section of ^{59}Co Below 36 MeV”, Journal of the Korean Physical Society, Vol. 59, No. 2, August 2011, pp. 18011804, DOI: 10.3938/jkps.59.1801

5) M. Majerle, et al., “Au, Bi, Co and Nb cross-section measured by quasi monoenergetic neutrons from p + ^{7}Li reaction in the energy range of 18-36 MeV”, Nuclear Physics A 953 (2016) 139-157. DOI: 10.1016/j.nuclphysa.2016.04.036.

6) M. Majerle, et al., “^{nat}Cu and ^{nat}V cross-sections measured by quasi-monoenergetic neutrons from p+^{7}Li reaction in the energy range of 18–34MeV”, EPJ Web of Conferences 146, 09019 (2017), DOI: 10.1051/epjconf/201714609019

7) M. Majerle, et al., “Cross sections measured by quasi-monoenergetic neutrons”, Radiation Protection Dosimetry (2018), Vol. 180, No. 1–4, pp. 386–390, DOI:10.1093/rpd/ncy031

8) H. Xiaolong, Nuclear Data Sheets for A = 196*, Nuclear Data Sheets 108 (2007) 1093-1286. DOI:10.1016/j.nds.2007.05.001.

9) M. Majerle, et al., “The intensities of γ-rays from the decay of ^{196m2}Au”, Applied Radiation and Isotopes **141** (2018) 5–9, DOI: 10.1016/j.apradiso.2018.07.026

10) S.D. Schery, et al., Activation and angular distribution measurements of ^{7}Li(p, n)^{7}Be(0.0+0.49 MeV) for E_p=25-45 MeV: A technique for absolute neutron yield determination, Nucl. Instrum. Methods Phys. Res. 147 (1977) 399-404, EXFOR B0127, doi:10.1016/0029-554X(77)90275-0

11) Y. Uwamino, et al., High-energy p-Li neutron field for activation experiment, Nucl. Instrum. Methods Phys. Res. **A389** (1997) 463-473, EXFOR E1826, doi:10.1016/S0168-9002(97)00345-8.

12) C.J. Batty, et al., “The ^{6}Li(p,n)^{6}Be and ^{7}Li(p,n)^{7}Be reactions at intermediate proton energies”, Nucl. Instrum. Methods Phys. Res. **A120** (1968) 297-320

13) H. Orihara, et al., “Status of the CYRIC neutron TOF facilities upgrade”, Nucl. Instrum. Methods Phys. Res. **A257** (1987) 189-196.

14) C.H. Poppe, et al., “Cross sections for the ^{7}Li(p,n)^{7}Be reaction between 4.2 and 26 MeV”, Phys. Rev. C **14/2** (1976) 438-445.

15) T.N. Tadeucci, et al., “Zero-degree cross-sections for the ^{7}Li(p,n)^{7}Be(g.s.+0.43-MeV) reaction in the energy range 80-795 MeV”, Phys. Rev. C **41/6** (1990) 2548-2555.

16) MCNPX 2.7.0. URL https://rsicc.ornl.gov/codes/ccc/ccc8/ccc-810.html

17) S.G. Mashnik, et al., LANL Report LA-UR-00-167 (2000).

M.B. Chadwick, et al., Nucl. Sci. Eng. **131**, 293 (1999).

18) S. Kunieda et al., "Overview of JENDL-4.0/HE and benchmark calculation" JAEA-Conf 2016-004, pp. 41-46 (2016).

19) SAND-II-SNL Neuron Flux Spectra Determination by Multiple Foil Activation-iterative Method, RSICC Shielding Routine Collection PSR-345, Oak Ridge 1996

20) D.E. Cullen, PREPRO 2010 - 2010 ENDF-6 Pre-processing Codes, Technical report IAEA-NDS-39 (Rev.14), International Atomic Energy Agency, Vienna, Austria

Nuclear Data Section
International Atomic Energy Agency
Vienna International Centre, P.O. Box 100
A-1400 Vienna, Austria

E-mail: nds.contact-point@iaea.org
Fax: (43-1) 26007
Telephone: (43-1) 2600 21725
Web: http://nds.iaea.org